International Journal of High-Rise Buildings
September 2014, Vol 3, No 3, 223-230

International Journal of
High-Rise Buildings
www.ctbuh-korea.org/ijhrb/index.php

Progressive Collapse and Seismic Performance of Twisted Diagrid Buildings

Kwangho Kwon[1] and Jinkoo Kim[2†]

[1]*Hyundai Architects & Engineers Associates Co., Ltd, Seoul, Korea*
[2]*Dept. of Civil and Architectural Engineering, Sungkyunkwan University, Suwon, Korea*

Abstract

In this study the progressive collapse resisting capacities of tall diagrid buildings were evaluated based on arbitrary column removal scenario, and the seismic load-resisting capacities were investigated through fragility analysis and ATC 63 procedure. As analysis model structures both regular and twisted diagrid structures were designed and their load-resisting capacities were compared by nonlinear static and dynamic analyses. The analysis results showed that the progressive collapse potential of twisted buildings decreased as the twisting angle increased, but the seismic fragility or the probability of failure decreased as the twisting angle increased.

Keywords: Progressive collapse, Seismic performance, Irregular structures, Diagrid structures

1. Introduction

Recently the geometric complexity and irregularity in tall building configuration have been rapidly increasing. Scott et al. (2007) explored the structural challenges that are created by buildings with unique geometries or articulated forms, and discussed economic design and construction techniques. Vollers (2008) categorized the geometry of high-rise buildings into *Extruders, Rotors, Twisters, Tordos, Transformers*, and *Free Shapers* depending on their form-generation method. Sarkar et al. (2010) proposed a new method of quantifying irregularity in building frames with vertical geometric irregularity accounting for dynamic characteristics, and provided a modified empirical formula for estimating fundamental period. Kim and Hong (2011) estimated the progressive collapse potential of tilted irregular buildings, where it was observed that the performance of irregular buildings subjected to sudden loss of a column depends significantly on the location of the removed column.

Among the irregularities of the vertical building forms, twisted building configuration has been applied to various major tall building projects including the *Turning Torso* in *Malmö*, *Infinity Tower* in *Dubai*, the *Chicago Spire* project, etc. In this study the progressive collapse resisting capacities of twisted diagrid buildings were evaluated based on arbitrary column removal scenario, and the seismic load-resisting capacities were investigated through ATC 63 (2009) approach and fragility analysis. As analysis model structures both regular and twisted diagrid structures were designed per Korean Building Code (KBC, 2009) and their load-resisting capacities were compared by nonlinear static and dynamic analyses.

†Corresponding author: Jinkoo Kim
Tel: +82-31-290-7563; Fax: +82-31-290-7570
E-mail: jkim12@skku.edu

2. Design of Analysis Model Structures

The prototype analysis model structure is a 36-story steel diagrid structure with square plan shape as shown in Fig. 1. For the purpose of comparison of structural performance, variations were made by twisting the prototype structure by 90°, 180°, and 270°, which are depicted in Fig. 2. The structures were designed per Korea Building Code (KBC, 2009) in such a way that the interior moment frames resist only gravity load and the lateral loads are resisted by the exterior diagrid system. The interior frames were designed using H shaped rolled sections and the exterior diagrids were designed with hollow sections. The design dead and live loads are 6 kN/m^2 and 2.5 kN/m^2, respectively, and the coefficients used for estimation of the design wind and earthquake loads are denoted in Table 1 and 2, respectively. As the diagrid system is not categorized as one of the seismic load resisting systems in most design codes, the response modification factor of 3.0 was used in the estimation of design seismic load. Table 3 shows the member sizes of the exterior diagrid frames of the four model structures at selected stories. It was observed that, in case the structures are designed using the same loading conditions, the required steel tonnage and the fundamental natural period increase as the twisting angle increases. The maximum displacements of the model struc-

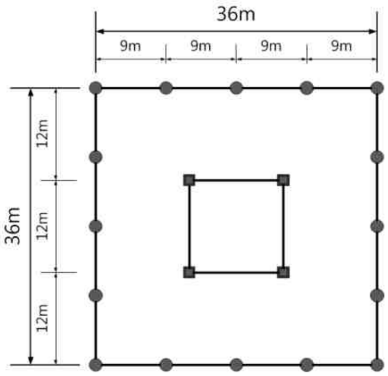


Figure 1. Structural plan of the model structures.

Table 1. Design wind load parameters

Basic wind speed	30 m/sec
Exposure	A (Downtown)
Importance factor	1.1

Table 2. Design seismic load parameters

Seismic coefficient (S)	0.22
Soil type	S_c
F_a	1.18
F_v	1.58
S_{DS}	0.433g
S_{D1}	0.232g
Response modification factor (R)	3.0
Importance factor (I_E)	1.2
Seismic design category	D

tures subjected to the design wind load were 15 cm (0°), 15.5 cm (90°), 17.9 cm (180°), and 23.31 cm (270°), respectively, which are less than the 1/500 of the total story height, which is 25.9 cm. As observed in Fig. 3, the maximum inter-story drifts of the model structures were within the limit value of 1.5% of the story height.

3. Progressive Collapse Resisting Capacity

A progressive collapse involves a series of local failures that lead to partial or total collapse of a structure. The progressive collapse resisting capacity of a building depends on the capability of the force redistribution including various factors such as redundancy, ductility, and configuration, etc. For structural design of structures against

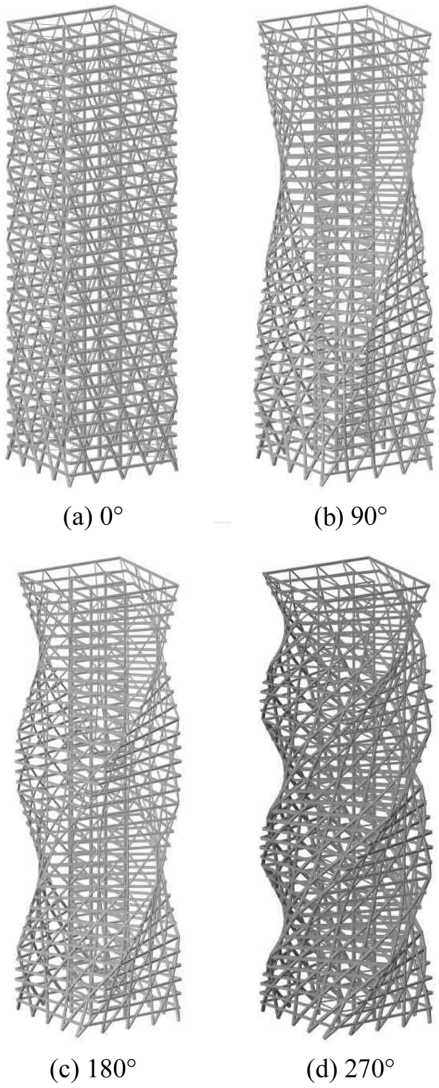


Figure 2. 36-story diagrid buildings with various twist angles.

progressive collapse, Alashker and El-Tawil (2011) proposed a design-oriented model for computing the load-resisting capacity of composite floors subjected to column loss. Recently a series of research was conducted to investigate the performance of building structures designed with various structure systems. Kim and Lee (2010) investigated the progressive collapse potential of tube-type structures, and Almusallam et al. (2010) evaluated the progressive collapse potential of a framed concrete buildings

Table 3. Member sizes of model structures at the selected stories (mm)

Stories	0°	90°	180°	270°
1-2	P 1016.0×12	P 1016.0×19	P 1025.0×30	P 1050.0×50
11-12	P 609.6×14	P 812.8×16	P 914.4×19	P 1030.0×25
21-22	P 500.0×14	P 600.0×16	P 609.6×22	P 914.4×22
31-32	P 406.4 ×9	P 457.2×9	P 406.4×19	P 700.0×12

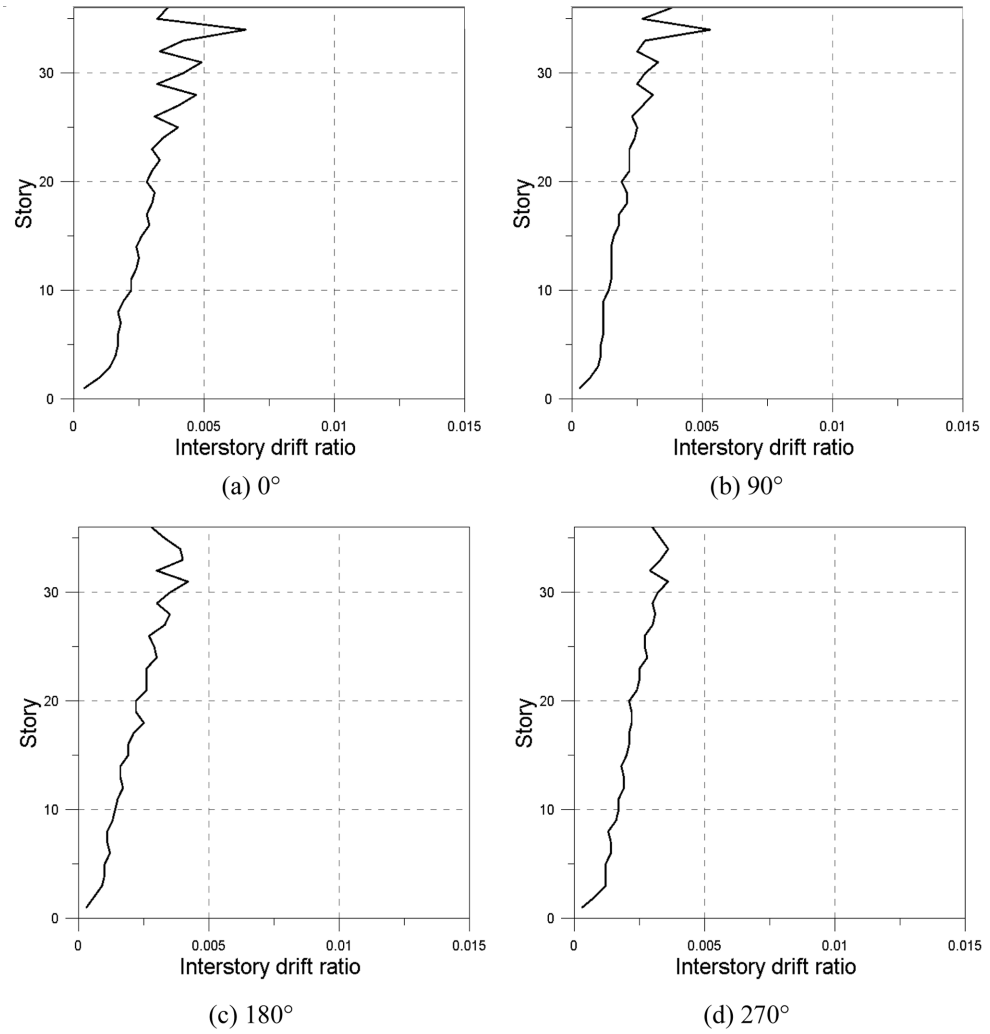


Figure 3. Maximum inter-story drifts of the model structures subjected to the design seismic load.

subjected to blast loads. Kim and Hong (2011) evaluated the progressive collapse performance of irregular buildings based on the arbitrary column loss scenario.

Fig. 4 shows the bending moment *vs*. rotation relationship of the structural elements recommended in the AS CE/SEI 41-06 (2007). The points *B* and *C* represent the nominal yield strength and the ultimate strength, respectively. The post-yield stiffness was assumed to be 3% of the initial stiffness. The points of *D* and *E* indicate the state of initial and the final failure, respectively. Also indicated on the curve are the performance limit states such as *IO* (immediate occupancy), *LS* (life safety), and *CP* (collapse prevention). The values of coefficients *a, b*, and *c* which define the nonlinear behavior can be found in ASCE/SEI 41-06.

Nonlinear static pushdown analyses of the model structures were conducted using the nonlinear analysis code SAP 2000 (2004) by arbitrarily removing vertical members of the structures shown in Fig. 5. The pushdown analysis results of the model structures subjected to removal

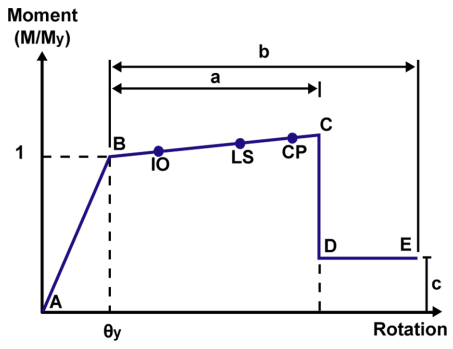
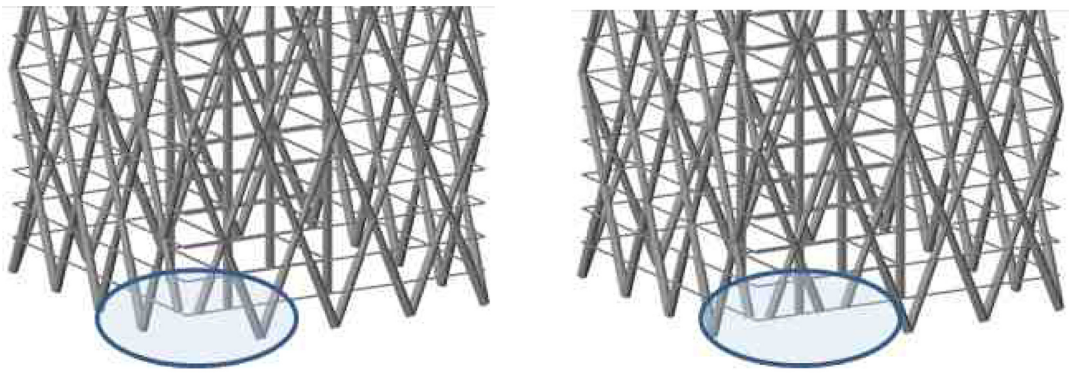


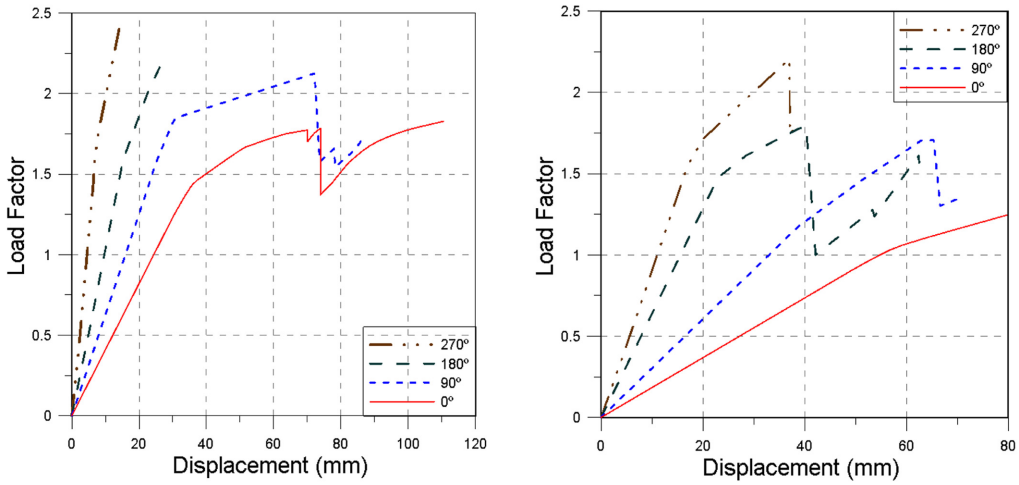
Figure 4. Nonlinear load-displacement relationship of bending members.

of a pair and two pairs of corner diagrids are shown in Fig. 6(a) and (b), respectively, where the load factor in the vertical axis represents the applied load divided by the initial member force. The figure shows that in every model structure the load factor exceeded 1.0, and therefore



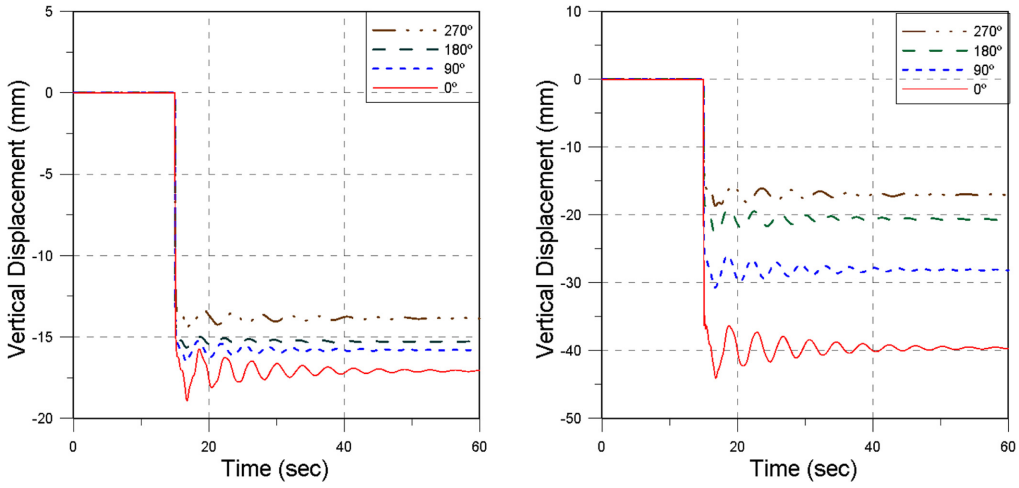
(a) A pair of diagrids (b) Two pairs of diagrids

Figure 5. Locations of removed diagrids.



(a) A pair of diagrids (b) Two pairs of diagrids

Figure 6. Nonlinear static pushdown analysis results for progressive collapse.



(a) A pair of diagrids (b) Two pairs of diagrids

Figure 7. Nonlinear dynamic analysis results.

the structures are safe for progressive collapse when one or two pairs of diagrids are removed from a corner. It also can be observed that as the twist angle increases the maximum load factor also increases, which implies that the progressive collapse resisting capacity increases as the twist angle increases. Fig. 7 depicts the nonlinear dynamic analysis results obtained by sudden removal of the first story corner diagrids, which shows that all the model structures remain stable after vertical vibration. The vertical displacements of the model structures after being stabilized turned out to be 17.05 mm, 15.79 mm, 15.28 mm, and 13.87 mm as the twist angle changes from 0 to 270, respectively, when a pair of diagirds were removed, and 39.75 mm, 28.17 mm, 20.62 mm, and 17.09 mm, respectively, when two pairs of diagirds were removed.

4. Seismic Performance Based on ATC 63

In this study the seismic performance and safety of the model structures were evaluated following the procedure recommended in ATC-63, in which collapse assessment is performed using nonlinear static (pushover) and nonlinear dynamic (response history) analysis procedures. Nonlinear static analyses are used to help validate the behavior of nonlinear models and to provide statistical data on system overstrength and ductility capacity, and nonlinear dynamic analyses are used to assess median collapse capacities and collapse margin ratios. Nonlinear response is evaluated for a set of pre-defined ground motions which include twenty-two ground motion record pairs from sites located greater than or equal to 10 km from fault rupture, referred to as the "Far-Field" record set. Nonlinear incremental dynamic analyses are conducted to establish the median collapse capacity and collapse margin ratio (*CMR*) for each of the analysis models. The ratio between the median collapse intensity, $\hat{S}_{CT}$, and the MCE intensity, S_{MT}, is defined as the collapse margin ratio (*CMR*), which is the primary parameter used to characterize the collapse safety of the structure. Fig. 8 depicts the schematic diagram for explaining the meaning of the collapse margin ratio (CMR) specified in ATC-63, which is obtained as follows:

$$CMR = \frac{\hat{S}_{CT}}{S_{MT}} = \frac{SD_{CT}}{SD_{MT}} \quad (1)$$

Collapse is judged to occur by dynamic instability. Using collapse data obtained from nonlinear dynamic analyses, a collapse fragility can be defined through a cumulative distribution function (CDF). The lognormal distribution is defined by two parameters, which are the median collapse intensity, $\hat{S}_{CT}$, and the standard deviation of the natural logarithm, β. The lowest intensity at which one-half of the records cause collapse is the median collapse intensity, $\hat{S}_{CT}$. The MCE intensity is obtained from the response spectrum of MCE ground motions at the fundamental period, *T*.

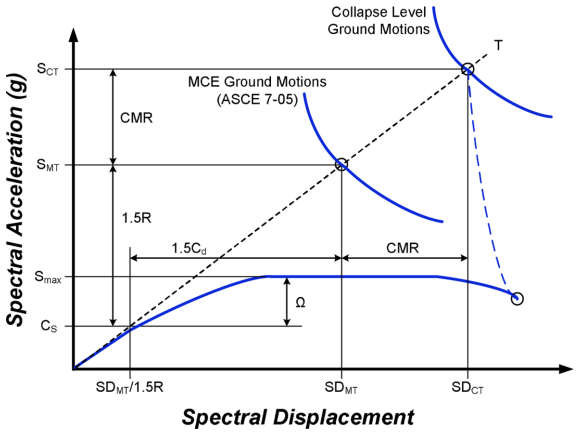


Figure 8. Schematic diagram for collapse margin ratio (CMR) specified in ATC-63.

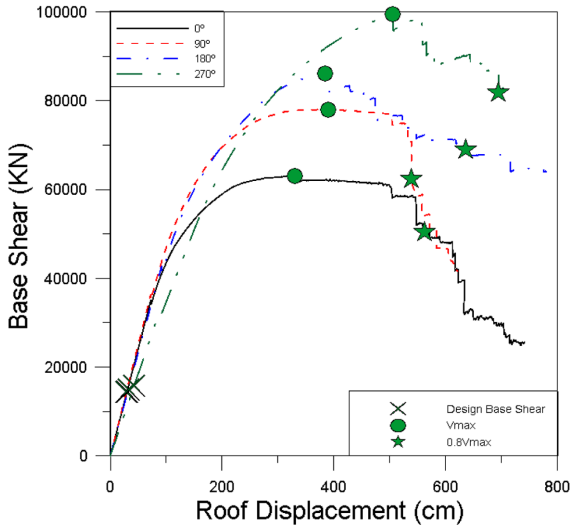


Figure 9. Seismic pushover analysis results of the model structures 3.

To account for the effect of spectral shape in determination of the collapse margin ratio, the spectral shape factors, *SSF*, which depend on fundamental period, *T*, and ductility capacity, μ_C, are used to adjust collapse margin ratios. The adjusted collapse margin ratio (ACMR) is obtained by multiplying tabulated *SSF* values with the collapse margin ratio that was predicted using the Far-Field record set. Acceptable values of adjusted collapse margin ratio are based on total system collapse uncertainty, β_{TOT}, and established values of acceptable probabilities of collapse. They are based on the assumption that the distribution of collapse level spectral intensities is lognormal, with a median value, $\hat{S}_{CT}$, and a lognormal standard deviation equal to the total system collapse uncertainty, β_{TOT}.

$$\beta_{TOT} = \sqrt{\beta_{RTR}^2 + \beta_{DR}^2 + \beta_{TD}^2 + \beta_{MDL}^2} \quad (2)$$

Table 4. Nonlinear static analysis results (KN, cm)

	V_{design}	V_{max}	Ω_0	$\delta_{y,eff}$	δ_u	μ_T
0°	14522.5	63000.02	4.338	136.71	561.65	4.11
90°	14489.75	78036.51	5.386	166.33	538.23	3.24
180°	15011.54	86170.63	5.740	200.20	635.84	3.18
270°	15764.23	99483.50	6.311	301.15	694.45	2.31

The total system collapse uncertainty is a function of record-to-record (RTR) uncertainty, design requirements related (DR) uncertainty, test data-related (TD) uncertainty, and modeling (MDL) uncertainty. Values of total system collapse uncertainty, β_{TOT}, are provided in Table 7-2 of the ATC-63. Table 7-3 of the ATC-63 provide acceptable values of adjusted collapse margin ratio, *ACMR10%* and *ACMR20%*, based on total system collapse uncertainty and values of acceptable collapse probability, taken as 10% and 20%, respectively.

Fig. 9 and Table 4 show the nonlinear static pushover analysis results of the analysis model structures using PERFORM 3D (2007). The lateral loads proportional to the fundamental mode shapes of the model structures were applied to the structures and the roof displacements and the corresponding base shears were plotted in the figure. The design base shear, maximum strength, and the failure point at which the base shear is reduced to 80% of the maximum strength are also indicated in the figure. It can be observed in the figure that the overstrength increases as the twist angle increases. However the ductility, which is the ratio of the maximum displacement and the yield displacement, decreases as the twist angle increases.

Fig. 10 depicts the incremental dynamic analysis results

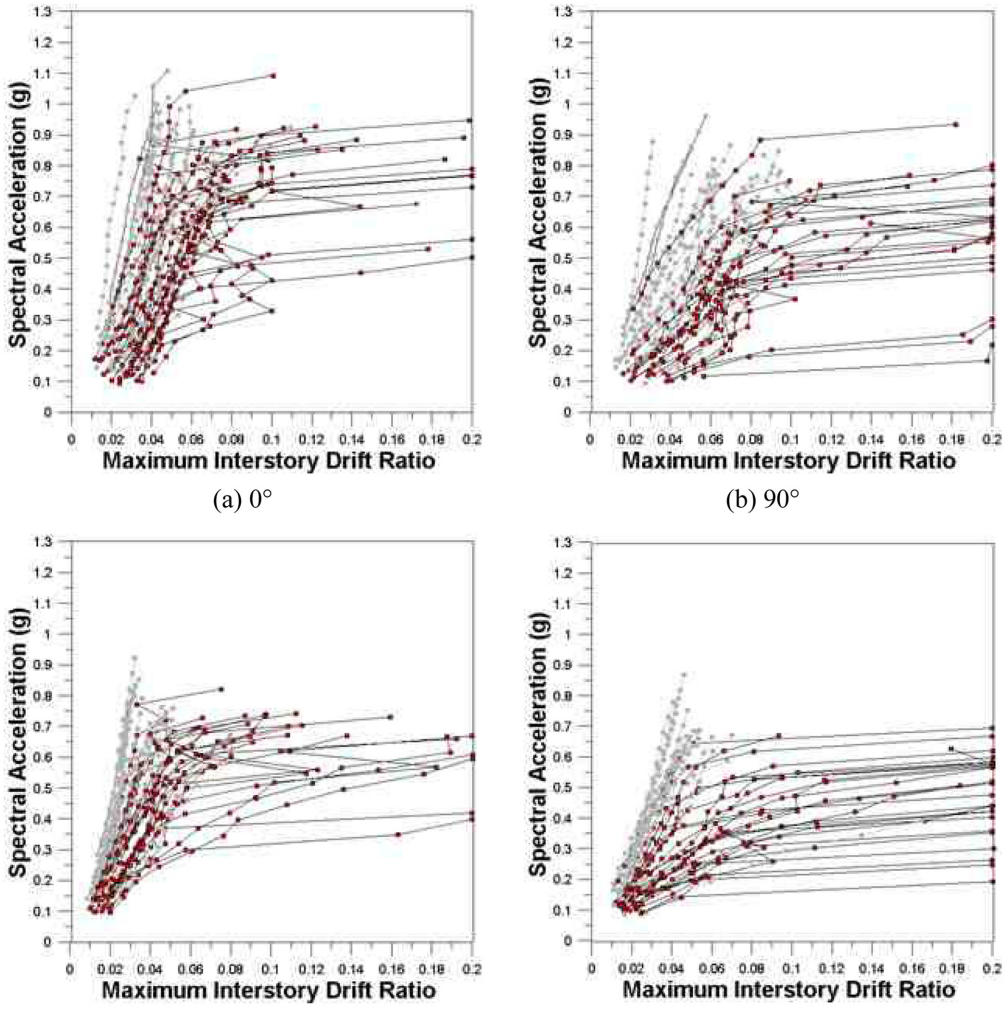


Figure 10. Incremental dynamic analysis results of the model structures with various rotation angles.

Table 5. Results of nonlinear incremental dynamic analysis results

	S_{MT}	$\hat{S_{CT}}$	CMR	SSF	ACMR	β_{TOT}	$ACMR_{20\%}$	Pass / Fail
0°	0.106	0.924	8.746	1.254	10.966	0.750	1.88	Pass
90°	0.107	0.787	7.381	1.220	9.002	0.750	1.88	Pass
180°	0.100	0.738	7.346	1.217	8.942	0.750	1.88	Pass
270°	0.088	0.567	6.443	1.169	7.529	0.725	1.84	Pass

of the model structures subjected to the 44 earthquake records obtained from the PEER NGA Database and normalized in such a way that the spectral accelerations corresponding to the natural frequency of the model structures coincide with the MCE design spectra. Damping ratios of 5% were used for all vibration modes. The median collapse intensity or the spectral acceleration ($\hat{S_{CT}}$) at which dynamic instability of each model structure was initiated by the 22nd earthquake record was determined from the IDA curves. The state of dynamic instability was defined as the point at which the stiffness of the structure decreased to 20% of the initial stiffness. Table 5 shows the adjusted collapse margin ratios (ACMR) of the model structures obtained from nonlinear incremental dynamic analysis results. It can be observed that the ACMRs of the model structures are much larger than the acceptable values of adjusted collapse margin ratio, ACMR20%, which implies that the response modification factor of 3.0 used for design of the model structures is valid. It also can be observed that the ACMRs decreases as the twist angle increase, which implies that the seismic safety against collapse decreases as the twist angle increases.

Fragility curves show the probability of a system reaching a limit state as a function of a seismic intensity measure. In this study pseudo spectral acceleration is used as the seismic intensity measure, and the seismic fragility is obtained from the incremental dynamic analysis results. The fragility is described by the conditional probability that the structural capacity, C, fails to resist the structural demand, D. It is generally modeled as a lognormal cumulative density function as follows (Vamvatsikos and Cornell 2002).

$$P[D<C] = 1-\Phi\left(\frac{ln[\hat{C}/D]}{\beta_C}\right) \quad (3)$$

where $\Phi[\bullet]$ = standard normal probability integral, $\hat{C}$ = median structural capacity associated with a limit state, D = median structural demand, β_C = system collapse uncertainty. The lognormal collapse fragility is defined by the median collapse intensity, $\hat{S_{CT}}$, and the standard deviation of the natural logarithm. The median collapse capacity corresponds to a 50% probability of collapse.

Fig. 11 shows the fragility curve for the model structures. The horizontal axis represents the seismic intensity corresponding to a certain level of collapse probability. FEMA-450 recommends that the assumed response modification factor is valid when the probability of collapse for the MCE-level earthquakes is less than 10%. The

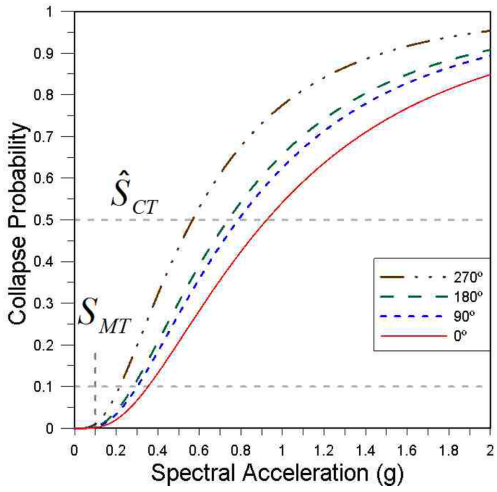


Figure 11. Fragility curves of the model structures.

figure shows that the collapse probabilities of the model structures corresponding to the spectral acceleration S_{MT}, which are shown in Table 5, are much less than 10%. Therefore it can be concluded that the model structures are generally safe against the MCE-level earthquakes and the response modification factor of 3.0 used for design of the model structures is valid. It also can be noticed that as the twist angle increases the seismic fragility, i.e., the probability of failure, also increases.

5. Summary

In this study the progressive collapse resisting capacities of 36-story twisted diagrid buildings were evaluated based on arbitrary column removal scenario, and the seismic load-resisting capacities were investigated through fragility analysis and ATC 63 procedure. The analysis results are summarized as follows:

The analysis model structures turned out to be safe against progressive collapse caused by arbitrary removal of one or two pairs of diagrids from the first story. It was also observed that the progressive collapse potential decreased as the twisting angle increased.

The adjusted collapse margin ratios (ACMR) of the model structures obtained from nonlinear incremental dynamic analysis results turned out to be much larger than the acceptable values of adjusted collapse margin ratio, ACMR20%, specified in the ATC 63, which implies that the response modification factor of 3.0 used for design of

the model structures is valid, It was also observed that the ACMRs decreased as the twist angle increased, which implies that the seismic safety against collapse decreases as the twist angle increases.

According to the fragility analysis the collapse probabilities of the model structures corresponding to the spectral acceleration S_{MT} are much less than 10%, which confirms that the model structures are generally safe against the MCE-level earthquakes. It was also observed that the seismic fragility decreased as the twisting angle increased.

Acknowledgements

This research was supported by a grant (13AUDP-B06 6083-01) from Architecture & Urban Development Research Program funded by Ministry of Land, Infrastructure and Transport of Korean government.

References

ASCE/SEI 41-06. (2007). Seismic Rehabilitation of Existing Buildings, ASCE Standard ASCE, American Society of Civil Engineers, Reston, Virginia.

ATC. (2009). Quantification of building seismic performance factors, ATC-63, Applied Technology Council, Redwood City, CA.

FEMA-450. (2003). NEHRP Recommended Provisions for Seismic Regulations for New Buildings and Other Structures, FEMA, Federal Emergency Management Agency, Washington, D.C.

Kim, J. and Hong, S. (2011). Progressive collapse performance of irregular buildings, *The Structural Design of Tall and Special Buildings*, 20(6), pp. 721~734

Korea building code, KBC 2009. (2009). Korea Architectural Institute.

PEER NGA Database. (2006). Pacific Earthquake Engineering Research Center, University of California, Berkeley, USA.

PERFORM-3D. (2006). Nonlinear analysis and Performance Assessment for 3D Structures-User Guide, Computers and Structures, Berkeley, CA.

Sarkar, P., Prasad, A. M., and Menonb, D. (2010). Vertical geometric irregularity in stepped building frames, *Engineering Structures*, 32, pp. 2175~2182.

SAP2000. (2004). Structural Analysis Program, Computers and Structures, Berkeley.

Scott, D., Farnsworth, D., Jackson, M., and Clark, M. (2007). The effects of complex geometry on tall towers, *Struct. Design Tall Spec. Build.*, 16, pp. 441~455.

Vamvatsikos, D. and Cornell, C. A. (2002). "Incremental Dynamic Analysis", *Earthquake Engineering and Structural Dynamics*, 31(3), pp. 491~514.

Vollers, K. (2008). Morphological scheme of second-generation non-orthogonal high-rises, *Proceeding of the CTBUH 8th World Congress 2008*, pp. 1~9.